RESULTS OF REACTOR-MATERIAL FUEL DISPERSAL TESTS GAP-3 AND GAP-4

by

B. W. Spencer, D. L. Vetter, R. Wesel, J. J. Sienicki

ABSTRACT

The results of reactor-material experiments are reported in which molten fuel drainage through mocked-up intersubassembly gap geometry was investigated. These tests relate to early fuel removal from the disrupted core during the meltout stage of the hypothetical core-disruptive accident in an LMFBR. The gap width was prototypic, 4.3 mm, the structure initial temperature was 1170°K, and the gap channel was voided (dry) for these gravity drainage tests; the molten fuel was a mixture of UO_2 (81%) and molybdenum (19%) generated by a thermite reaction at 3470°K. In the GAP-3 test, the injected molten fuel was immobilized by freezing at a penetration distance of 0.18 m. The plugging in this test was apparently due to solidification of the molybdenum which had segregated to the leading edge. In the GAP-4 test, the UO_2/Mo mixture was homogeneous, and the penetration distance was 0.35 m.

SUMMARY

Tests have been performed examining the penetration behavior of molten reactor materials through flow path geometries mocking up the gaps between subassemblies in the CRBR hetrogeneous core design. These tests relate to the ability of molten core materials to be dispersed from the core early in the meltout stage of the hypothetical core disruptive accident. The two tests described were performed under nominally identical conditions, namely i) gravity draining through a heavy-walled, 2-D rectangular channel, ii) 4.3 mm gap dimension, iii) 1170°K initial structure temperature, and iv) 2 kg molten fuel mass. The fuel melt was generated by a thermite reaction and consisted of 81% UO_2 and 19% Mo at an initial temperature of 3470°K. In the GAP-3 test a prolonged reaction time of ∿ 15 s resulted in segregation of the metallic molybdenum and oxdic UO_2 constituents in the reaction vessel prior to injection. The result was that the molybdenum entered the gap test section first and froze forming a complete plug at a penetration distance of 0.18 m. In GAP-4 the reaction time was reduced to ∿ 3 s and the constituents remained well homogenized upon injection with the result that the leading edge penetration distance increased to 0.35 m. The test results showed the presence of stable, insulating fuel crusts on the steel walls; there was only localized melting and ablation of the walls. Although these observations are consistent with the stable-crust, conduction-limited model of heat transfer controlling the fuel freezing process, application of this model to the test conditions results in calculated penetration distances in excess of 1 m, considerably longer than found in the experiments. Although factors contributing to shorter penetration depths were examined analytically, namely i) lack of superheat in the thermite reactants, ii) radiation heat loss from the leading edge, and iii) the cooling effect of blowby gas, none of these individual effects appears satisfactory at explaining the measured penetration behavior.

I. INTRODUCTION

A. Background

One of the key issues which arise in the assessment of the meltout phase of the hypothetical core disruptive accident in the LMFBR system involves the timing and paths for molten fuel to escape from the disruptive core. The earliest available paths are through the axial blankets where, depending upon the specific accident sequences considered, the flow channels may be initially open to above the tops of the pins and perhaps to below the bottoms of the pins. An extensive test program has been carried out examining the molten fuel penetration behavior axially through pin bundle structure for varying conditions of structure temperature, mass of molten fuel, injection pressure, and injection flow regime [1-3]. These tests have generally shown that the available injected fuel mass can be relocated into the axial pin structure, but that it is unlikely that it will pass entirely through the pin length to the open pool regions beyond. The injected fuel has typically come to rest and solidified within the pin structure, creating plugs. These plugs have been generally complete (impervious to gas passage) for large injection mass cases but have generally exhibited sufficient interconnected porosity to allow gas passage for the small mass cases. The plug compositions have indicated that a high rate of cladding melting and entrainment occurred during the fuel passage time with the effect that resolidified steel was a major portion of the plugs.

The disrupted subassembly geometry confined by axial plugs is only a temporary state since decay heating in the fuel in the plugs will eventually cause the plugs to remelt. Additional axial dispersal may then be possible at the prevailing subassembly pressure. This process of plug remelting is estimated to require 10's of seconds. During this time, the core power generation results in additional fuel melting as well as internal pressurization due to gas release, steel vaporization, and perhaps fuel vaporization. The restraining hexcan walls will heat up, and it is estimated that they will reach melting in a time scale of $\sim$ 2-4 s, far sooner that the axial plugs are expected to melt out [4].

The significance of this is that additional paths for fuel escape from the core are expected to become available as the hexcan walls lose their structural integrity. Possible fuel escape paths which have been identified include: i) the gaps between the hexcans leading to the below-core volume via drainage, ii) the intersubassembly gaps as a path for pressure-driven expulsion into the radial blanket and shield assembly region, iii) blowdown and/or drainage through the relatively wide-open control rod (CR) assemblies, and iv) paths opened by removal of structure such as upper hexcan stubs. Some of all of these removal paths are expected to become available during the hexcan meltout stage prior to the disruptive region achieving core-wide coherency.

The first removal path to become available during the meltout stage involves the narrow channels separating the hexcan walls; i.e., the intersubassembly gaps. In the unirradiated, cold condition the hexcan-to-hexcan pitch allows for a gap between hexcan walls of 4.7 mm. This spacing, illustrated in Fig. 1, is held nominally uniform by the bearing pads on the hexcan flats. The gaps are filled with sodium which is essentially stagnant, although there is some leakage flow through the lower support plate structure and past the load pads. The pressure in this region is the upper plenum cover gas pressure plus static head. The nominal area of this gap region is $\sim$ 8% of the core cross-sectional area, and this area is available for fuel drainage down as low as the core support plate.

During reactor operation the gap sizes will vary from location-to-location across the core and axially due both to irradiation-induced swelling as well as "circumferential" growth by thermal expansion. Calculations indicate that the gaps may close completely between adjacent driver assemblies in the peak fluence regions at end-of-life [5]. Wall heatup during a loss-of-flow accident has the effect of additionally closing the gaps between adjacent driver assemblies, although the corners between hexcans are expected to remain open. Also, the gaps remain open in regions of lower temperature and/or lower fluence such as i) below the active core, ii) in the radial blanket and shield regions, and iii) between adjacent control rod (CR) and internal blanket (IB) assemblies.

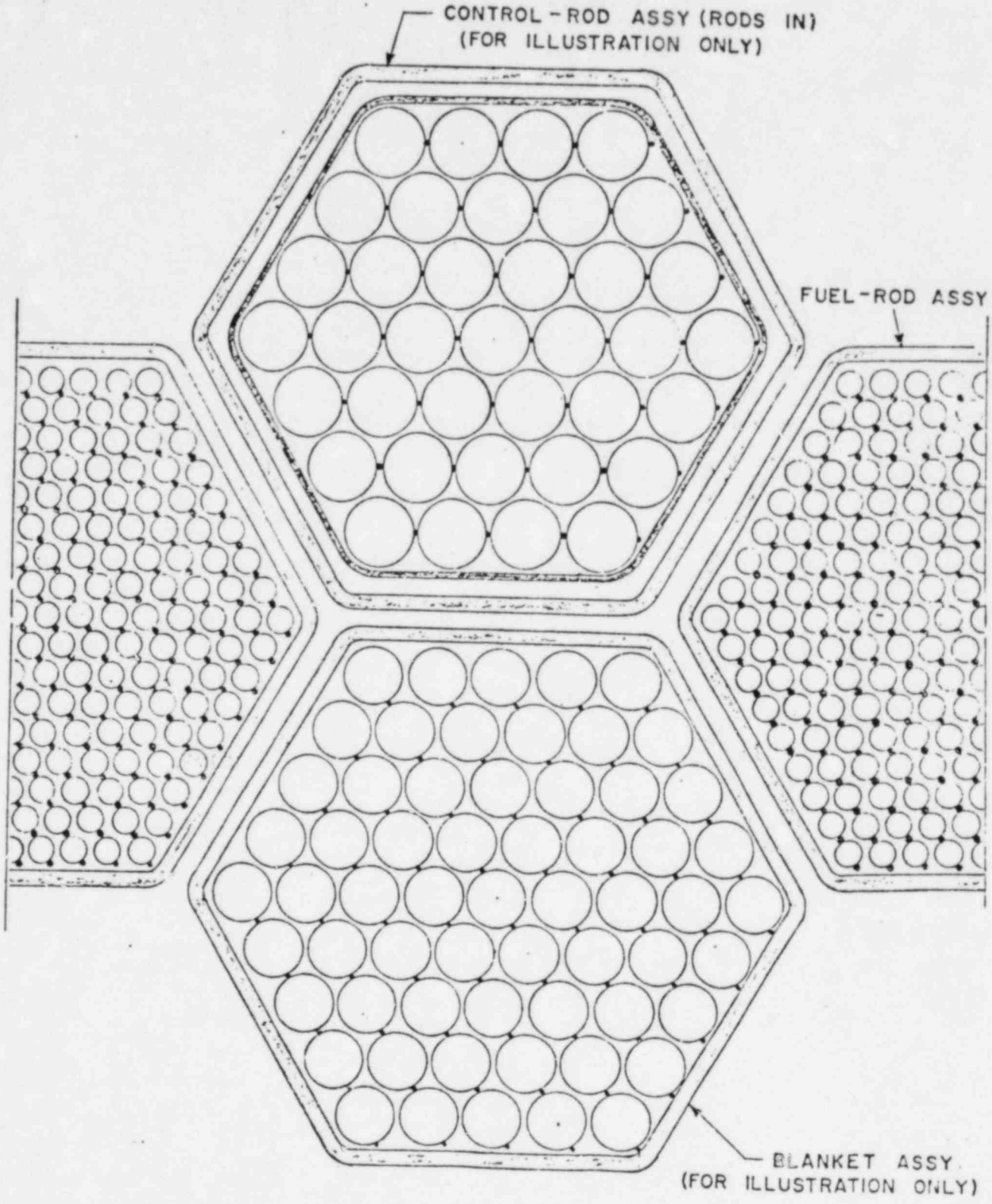

Figure 1. Illustration of Intact-geometry Hex Duct Cross Sections in CRBR Hetrogeneous Core

Tests have recently been performed at ANL which indicate that the hexcan can be expected to fail initially by a narrow crack forming at one of the corners [6]. The failure temperature for internal pressures of 5-10 atm has been found to be within ∿ 100°C of the wall melting temperature when the walls are restrained against large deformation by the presence of adjacent hex ducts in reactor geometry. It is anticipated that the crack-like corner failure of the disrupted driver assembly would initiate a two-phase molten fuel/gas/vapor blowdown through the breach, and that canwall ablation would soon result in a large opening for fuel to escape. Although not all boundary failures will provide fuel entry into open escape paths due to gap closures, eventually the open volumes between CR/IB and IB/IB assemblies will be accessed, and subsequently the open volume beneath the active core and in the RB region will also be accessed. The former case is illustrated in Fig. 2 where a disrupted SA is depicted undergoing blowdown into the open volume between adjacent CR and IB assemblies. The distance the fuel may disperse in the radial direction is limited in this case by the closed gaps past the first corner, but the molten fuel that enters this region has an open path to drain downward into the large interconnected gap volume beneath the core.

B. Objectives

The purpose of this investigation was to examine the penetration distances of molten fuel flowing through the narrow, two-dimensional channels representing the intersubassembly gap geometry. The freezing-limited penetration behavior has been decoupled in this investigation from the associated processes of hexcan failure, wall ablation, and SA blowdown. (An integral test of this kind is in the development stage.) The specific objective of this work relates to determination of the maximum penetration distance of the fuel flowing through the gap given its entrance into the gap, together with comparison between experiment results and predictions based upon fuel freezing models.

C. Approach

An experiment apparatus was constructed to mock up the 2-D internal flow path of the intersubassembly gaps. The walls of the flow channel

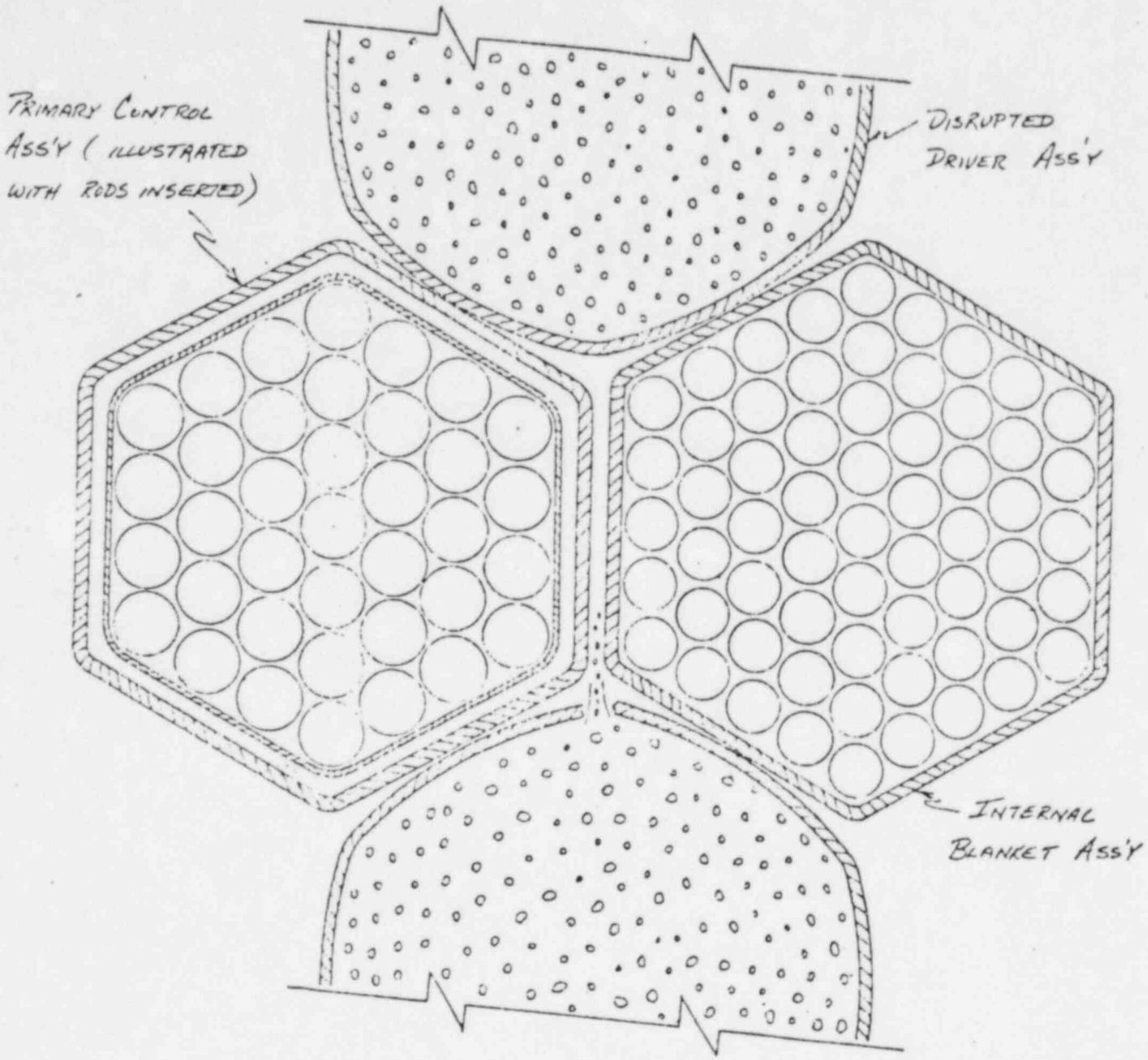

Figure 2. Illustration of Initial Disruption Process Involving Molten Fuel Entering Intersubassembly Gap Volume

were made thick in order to avoid anaomlous distorsion of the gap thickness by transient heating effects. Pretest calculations were performed which indicated that the wall thickness had negligible influence on the heat flux into the wall or the leading edge penetration distance for the time duration of these tests. The tests were performed dry (i.e., without the presence of sodium liquid or sodium film on the channel surface) since calculations indicated that the gaps in the active fuel region would void prior to hexduct meltout [5]. A future test is planned to be performed with sodium to examine sodium vaporization effects in the nonvoided, below-core region.

The gap geometry was selected to be two-dimensional on the basis that the gap volume in the reactor design is interconnected and continuous. Hence, outside the peak temperature and fluence regions where the gaps may be closed, fuel entering into the gaps will generally be able to spread laterally as it flows downward. This was accommodated in the experiment design by injecting the molten fuel across one "flat" width, 6.3 cm, and allowing the fuel to spread across $\sim$ 3 flats width, 20.3 cm. The gap thickness of 4.3 mm was selected on the basis of the thicknesses of the mating load pads. Although the nominal cold gap dimension is 4.7 mm based on the SA-to-SA pitch dimension of 120.9 mm, this includes $\sim$ 0.4 mm clearance at the load pads for SA insertion and removal. This clearance disappears at operating temperature so that the load pads determine the gap thickness [5]. The overall length of the gap path in the experiment design, 1.0 m, is the distance from the core midplane downward to the top of the shield zone where the SA-to-SA gap reduces to the clearance dimension.

The molten fuel used in these tests was a mixture of UO_2 (81%) and molybdenum (19%) and was generated by an exothermic thermite reaction at a temperature of $\sim$ 3470°K. This was the same fuel mixture used in the blanket penetration tests [1] although these gapflow tests were performed at much lower injection pressure. Although the SA blowdown process upon failure may result in carryout of liquid fuel in a dispersed flow regime, the geometry suggested by Fig. 2 was conservatively modeled as a separator in which the gas/vapor could disengage from the fuel and escape axially

while the molten fuel accumulated locally in the channel. The fuel removal process is then envisioned as a simple downward gravity draining. Hence the experiments were performed under nominally gravity drain conditions, although in reality this may be an overly restrictive assumption.

II. EXPERIMENT DESCRIPTION

A. Experiment Apparatus

The experiment apparatus used for the GAP fuel penetration tests is shown in Fig. 3. The apparatus consists of the following major components: 1) thermite injection assembly, 2) gas system used to control the injection conditions, 3) GAP test section, and 4) receiver tank.

A detail of the thermite injection vessel is shown in Fig. 4. The vessel is sized for a load of nominally 4 kg. The vessel walls are lined with a refractory material so that the vessel is reusable. The wedge-shaped liner at the bottom funnels the reaction products out the bottom of the vessel through a 2.54 cm dia circular opening controlled by a sliding member. A thin layer ($\sim$ 0.5 cm) of graphite powder was placed atop the slide; the reaction powders consisting of $U + \frac{2}{3} MoO_3$ were packed into the vessel to near the porous grid plate. The cover gas was argon. A nichrome heating element was coiled just beneath the upper surface of the powders; the exorthermic reaction was initiated by passing a current through the igniter wire. A twisted pair of magnet wires at the bottom of the vessel shorted when the reaction had propagated the full column height of the powders, and this contact closure was used to start the auto test sequence. The molten fuel was released by a sudden opening at the bottom effected by the slide actuation. The typical opening time was 16 ms.

Gas piping connected to the top of the vessel was used to control the vessel pressure both during the reaction and subsequently during the fuel release. The vent line, Fig. 3, led to a large accumulator volume to maintain a low, nominally ambient pressure. The pressure at injection was controlled by a separate reservoir tank in the pressurizer line.

The injector was separated from the test section by a 0.11 m-long cooling spool. This finned-member was needed to maintain the thermite reactants near room temperature while the test section was heated to 1170°K. The cooling spool had a tantalum liner with an ID of 2.44 cm. Between the cooling spool and the test section was a 0.09 m-long circular-to-rectangular transition piece which was fabricated from stainless steel

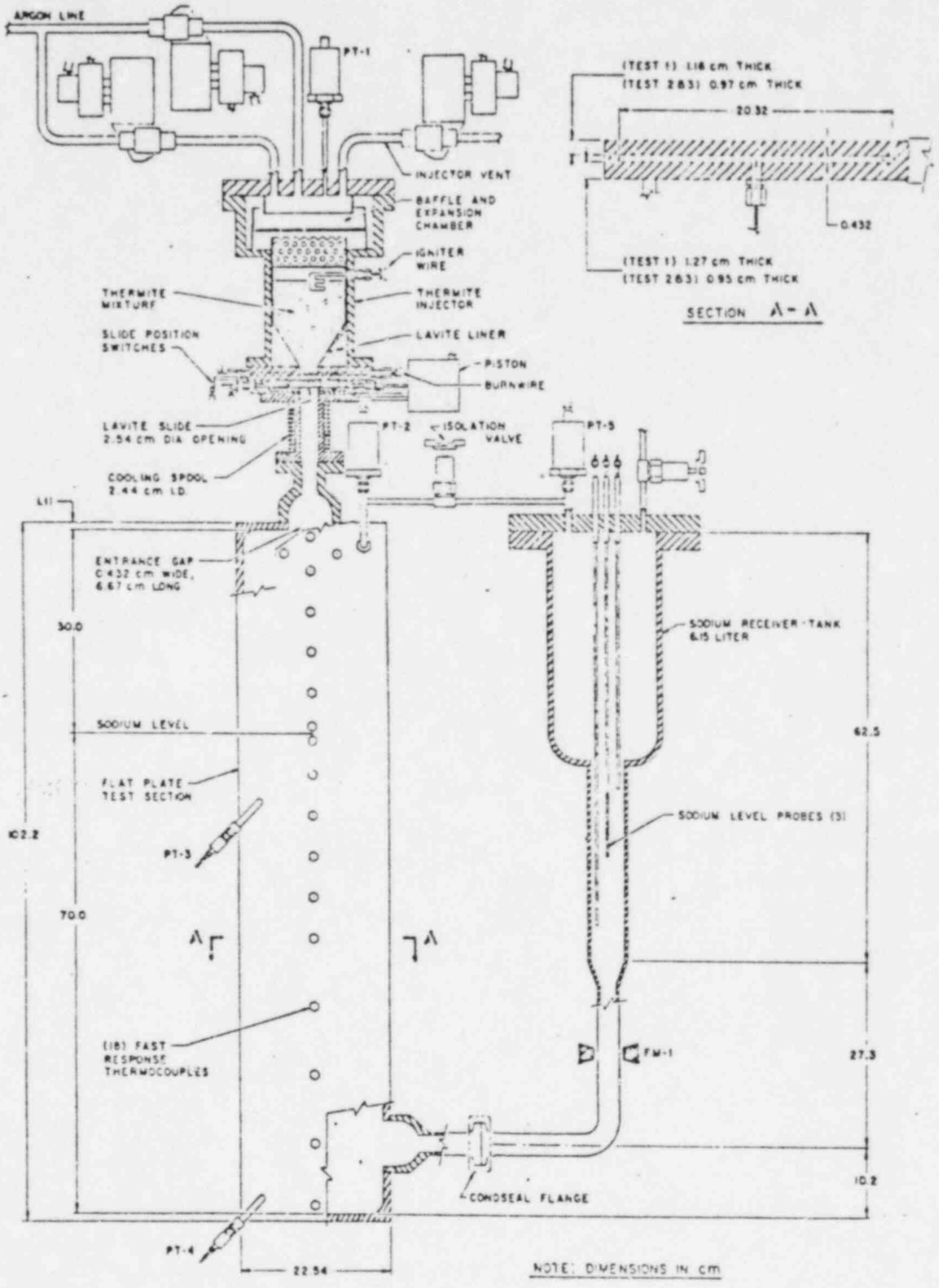

Figure 3. Experiment Apparatus used for Reactor-material Fuel Dispersal Tests in Intersubassembly Gap Geometry

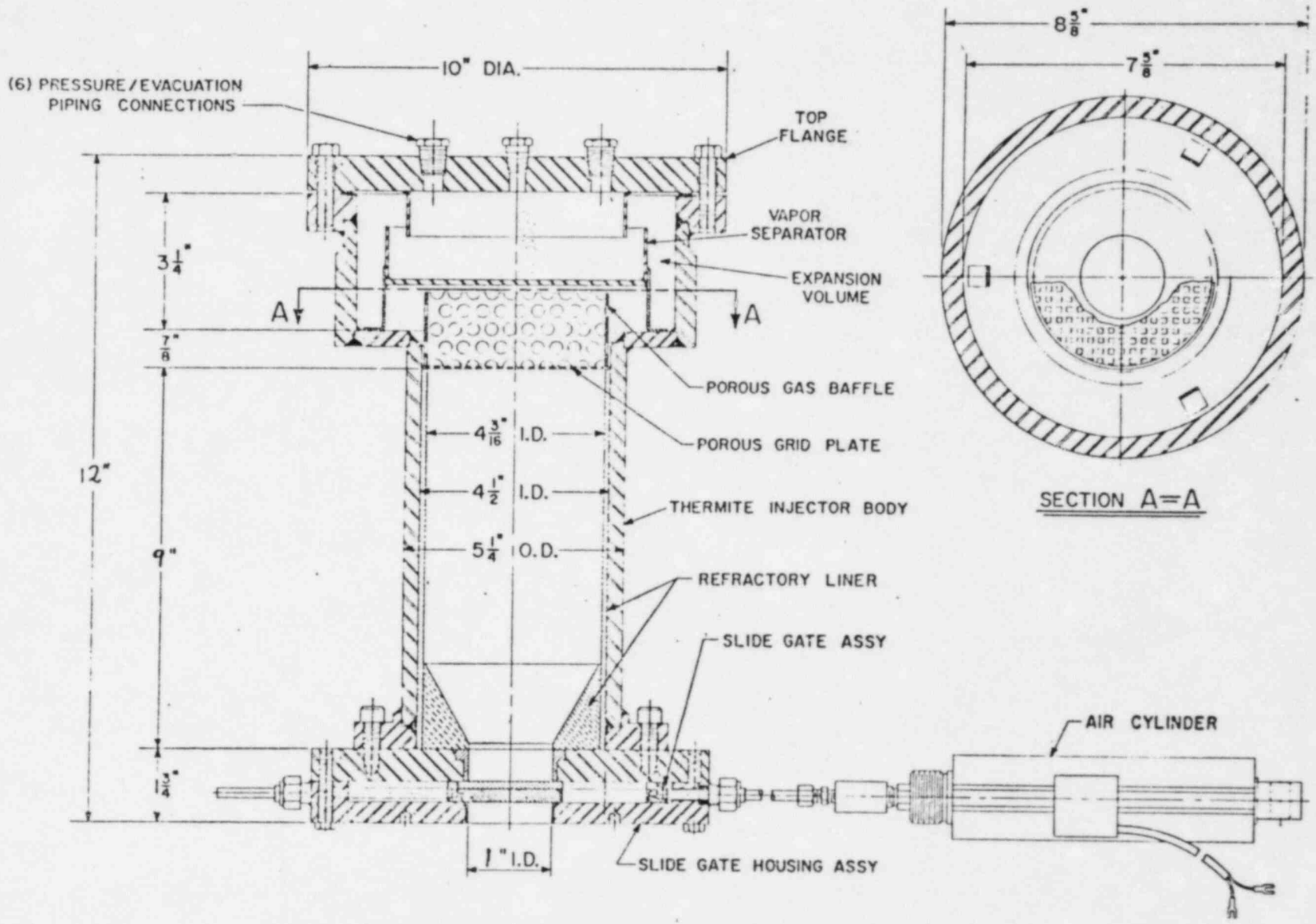

Figure 4. Detail of Thermite Reaction Vessel used for GAP Tests

using an EDM machining technique. The design maintains a constant cross-sectional area in going from the 2.54 cm dia circular path to the 0.43 x 6.7 cm rectangular path.

The test section is a simple structure comprised of two flat plates with milled recesses of one-half the gap width on each. The plates were placed atop one another and the joint was welded. The walls were ∿ 1 cm in thickness, and the gap dimension was 0.43 x 20.3 x 100 cm-long. Penetrations for internal thermocouples and pressure transducers were provided (Fig. 3). The test section was outfitted with trace heaters, surface TC's, and thermal insulation to allow for heatup to 1170°K.

A transition piece similar to that at the test section entrance was located near the bottom of the test section as shown in Fig. 3. This was intended to connect to a receiver tank for those tests in which sodium was present in the gap. Sodium was not used in the GAP-3 and GAP-4 tests described here, and the receiver tank was not as illustrated. However, a 8.5 l tank was used in its place which was connected to the bottom of the test section as illustrated. This tank provided volume for displaced fill gas as the molten fuel flowed downward through the test section.

B. Instrumentation

Strain-gage type pressure transducers were located at the thermite injector, test section, and receiver tank as well as various locations in the gas and slide systems. Those PT's on the injector and test section were mounted at the end of standoff tubes to protect them from transient heating effects and from direct contact by fuel; the standoff tubes were 0.7 cm ID by ∿ 7.5 cm long. In-stream TC's were placed along the centerline of the flow channel to monitor the fuel front progression. These Type-K TC's were used primarily as event indicators and were typically destroyed by the passage of the molten fuel. They were 0.25 mm OD, had grounded junctions, and extended ∿ 0.1 cm into the flowpath from the wall (see Section A-A in Fig. 3). Other miscellaneous instrumentation was used to control and record the event sequence.

Test data was recorded on-line using a Honeywell 1858 fibre-optic oscillographic recorder. Data was also recorded on a Honeywell 101

28-channel FM tape recorder. The data was recorded wide-band at a speed of 60 ips (40 kHz bandwidth). The data was digitized and processed on a PDP-11 computer, and hard copies were made of the data plots off the graphics display.

C. Experiment Procedure

The thermite reaction products were mixed and loaded into the injection vessel under argon cover gas in a specially-outfitted glove box. The injector assembly was installed atop the test section, the pipes were bled full of argon, and the piping connections were made under argon blanket. All valve positions were placed in a pretest standby condition. The test section heatup was initiated. A helium gas jet was directed onto the cooling spool to minimize conduction heat transfer to the thermite vessel. The test section was heated to 900^{+10}_{-25}°C using four temperature control zones. When the operating temperature was reached, excess gas pressure was vented from the test section, heater power was turned off (to minimize noise pickup), the data recorders were started, the current was turned on to the thermite igniter circuit, and the gas line valves to the vent accumulator tank were automatically opened.

The sequence timing for tests GAP-3 and GAP-4 are listed in Table 1. The burntime is the time from the igniter current ON to the shorting of the burnwire pair at the bottom of the vessel. The burnwire closure activated the sequence timer circuit. The time interval from 0 to T1 provided prolonged gas venting after the reaction was nominally completed. At time T1 the vent valves were closed isolating the injector vessel. The time interval from T1 to T3 provides a setting time for the molten pool to form. At time T3 the gas line valve to the pressurizer tank was opened. The time interval T3 to T4 allowed the system pressure to equilibrate at about the preset pressurizer tank pressure. At time T4 the gas line valve in the slide circuit was opened, pressurizing the slide piston, and initiating slide travel. Complete opening typically required $\sim$ 16 ms. This action initiated the fuel injection process. The pressure in the injector system remained constant during the injection process by action of a regulator in the pressurizer tank. The pressurizer valve was closed at 5 s later.

Following the test, the heater power remained off, and the system cooled to room temperature. The apparatus was disassembled and the injector, spool piece, and test section were weighed to determine weight changes. The mass of fuel which entered the test section was determined. The test sections were gammagraphed in order to observe the overall frozen fuel disposition. The test sections were cut through at selected zones in order to observe and photograph the frozen fuel cross sections. The chemical makeup of selected debris from GAP-3 was checked using the ANL scanning electron microscope (SEM).

TABLE. I. Sequence Timing for GAP Fuel Penetration Tests

	GAP-3	GAP-4
Burntime, s	14.3	2.86
Burnwire Closure, s	0.00	0.00
Isolate Injector Vessel (T1), s	2.50	0.20
Open Pressurizer Line (T3), s	3.25	0.25
Actuate Slide Travel (T4), s	3.30	0.30
Close Pressurizer Line, s	8.00	5.00

III. TEST RESULTS

Initial conditions for the GAP-3 and GAP-4 tests are summarized in Table 2. In both tests the structure temperature was initially 900°C. The injector was loaded with about 4 kg of reaction powders which was expected to deliver nominally 2 kg of the molten fuel mixture (81% UO_2 + 19% Mo @ 3470°K) into the test section.

A. GAP-3

The GAP-3 test was the first of the current series to investigate molten fuel penetration through the gap geometry under nominally gravity drain condition. The pressurizer tank was set to a slight positive pressure of 0.136 MPa (5 psig) in order to assure fuel entry into the test section and to preclude negative pressure in the injector as the fuel flowed out. The injector pressure at the onset of injection was 0.146 MPa (6.5 psig). The posttest gammagraph, Fig. 5, shows that the fuel leading edge penetrated ∿ 0.18 m through the gap channel. The responses of the internal TC's located along the fuel path are summarized in Fig. 6. The frontal velocity indicated from this data is ∿ 8.5 m/s, about an order of magnitude faster than a calculated all-liquid drainage velocity. This TC behavior is thought to result from an initial two-phase expansion of hot material from the injector which may have been followed by a more single-phase liquid flow. This behavior had been observed in 7-pin bundle test CRBR-6 in which both internal TC's and a flash x-ray system were used for diagnostics [1].

The posttest examination revealed that only 1.08 kg of the expected 2 kg of molten fuel material actually entered the test section. Based upon the completeness of the plug that was formed and the fact that it filled the upper corners of the test section, it appears that plugging was due to freezing at the leading edge in this test; the melt filled in behind the leading edge occupying the volume available to it. The thermite injector had not been emptied, and a slug of material filled the transition piece and cooling spool to the bottom of the injector. Hence it was concluded that failure to achieve the desired 2 kg of fuel

TABLE II. Conditions for Fuel Penetration Tests GAP-3 and GAP-4

	GAP-3	GAP-4
U Powder	B- 960 (24%) B-1000 (53%) B-1019 (23%)	B-1019 (100%)
Reactant Load, kg	4.10	3.83
Initial Structure Temp, °C	900	900
Pressurizer Tank, MPa (psig)	0.136 (5)	0.136 (5)
Initial Injection Pressure, MPa (psig)	0.146 (6.5)	0.150 (7)
Mass of Fuel Injected, kg	1.08	2.38
Leading Edge Penetration, m	0.18	0.35

GAP-3

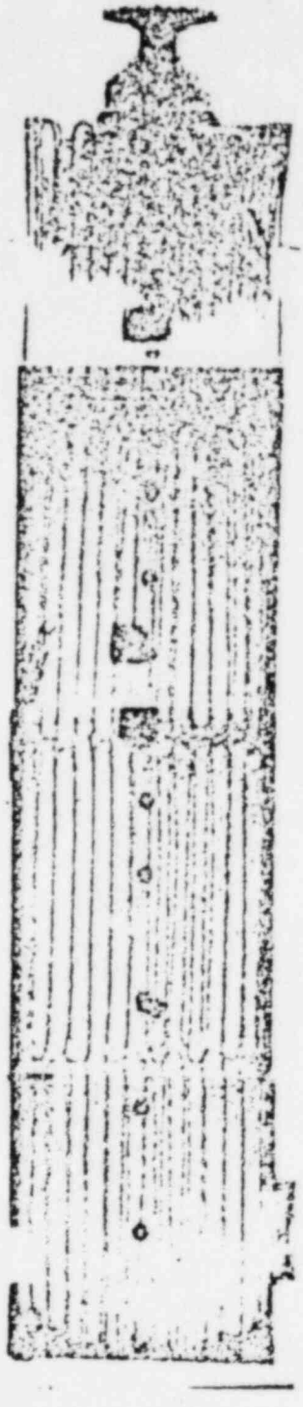

GAP-4

Figure 5. Posttest Gammagraphs from GAP-3 and GAP-4 Fuel Dispersal Tests

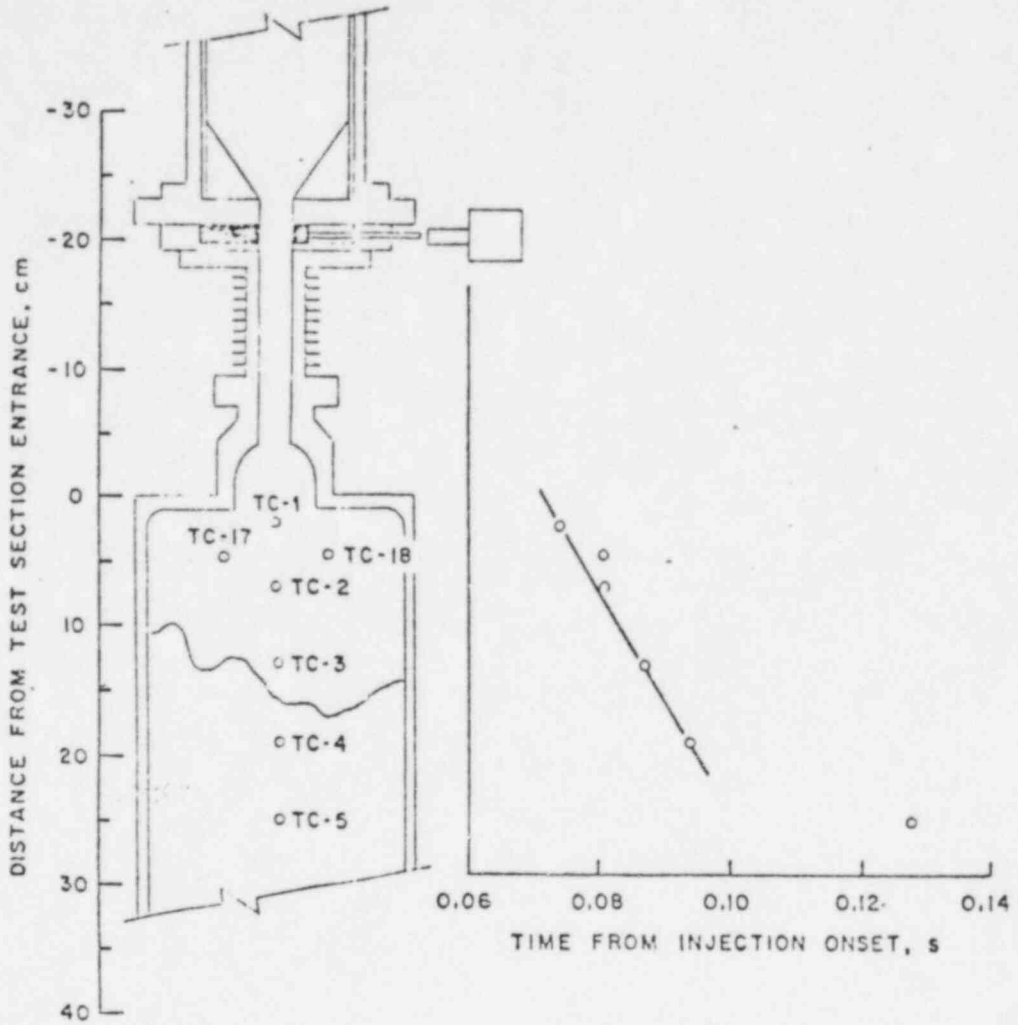

Figure 6. Thermocouple Data from GAP-3 Showing Leading Edge Travel Times

injection was caused by freezing and plugging of the fuel in the test section rather than too small a melt mass in the injector.

The test section was cut into sections for visual examination. A transverse cut was made at 0.205 m, beyond the frozen fuel mass, and an axial cut was made through the full length of the plug at 1.0 cm off the centerline (adjacent to the TC penetrations). The cut, shown in Fig. 7, showed that the gap was essentially solidly filled from the leading edge back to the transition piece, although some macroscopic voids were present. There was no sign of any significant melting of the steel walls, and fuel crusts were present on the steel surface in regions where significant fuel had flowed past. The appearance of the solidified debris was unusual in this test in the sense that considerable agglomeration and segregation of the molybdenum from the UO_2 was apparent. The metallic material was concentrated at the leading edge. A chunk of the metallic material was taken from the leading edge, and examination by the scanning electron microscope (SEM) verified that the material was molybdenum. An SEM analysis of material taken from the top of the gap indicated nearly all UO_2 with very little Mo present. The segregation exhibited in this test is in contrast to previous fuel freezing tests in which the Mo tended to remain as a finely-dispersed constituent in the UO_2.

The large degree of segregation between the metallic and oxidic constituents of the fuel melt in this test is regarded as an anomaly which may have had an effect of shortening the penetration distance. The reason for this segregation is thought to have been the combination of a long burntime (14.3 s) in the thermite mixture together with a relatively long settling time of 3.3 s prior to initiating the injection. Previous tests in which thermite reactions had taken place with failure to initiate injection had shown a similar segregation of the oxidic and metallic constituents in the solidified ingot, characteristically showing the metallic component at the bottom of the ingot. In GAP-3, it is speculated that the agglomeration and segregation processes had been underway prior to the onset of injection and that molybdenum was the first material to enter the test section.

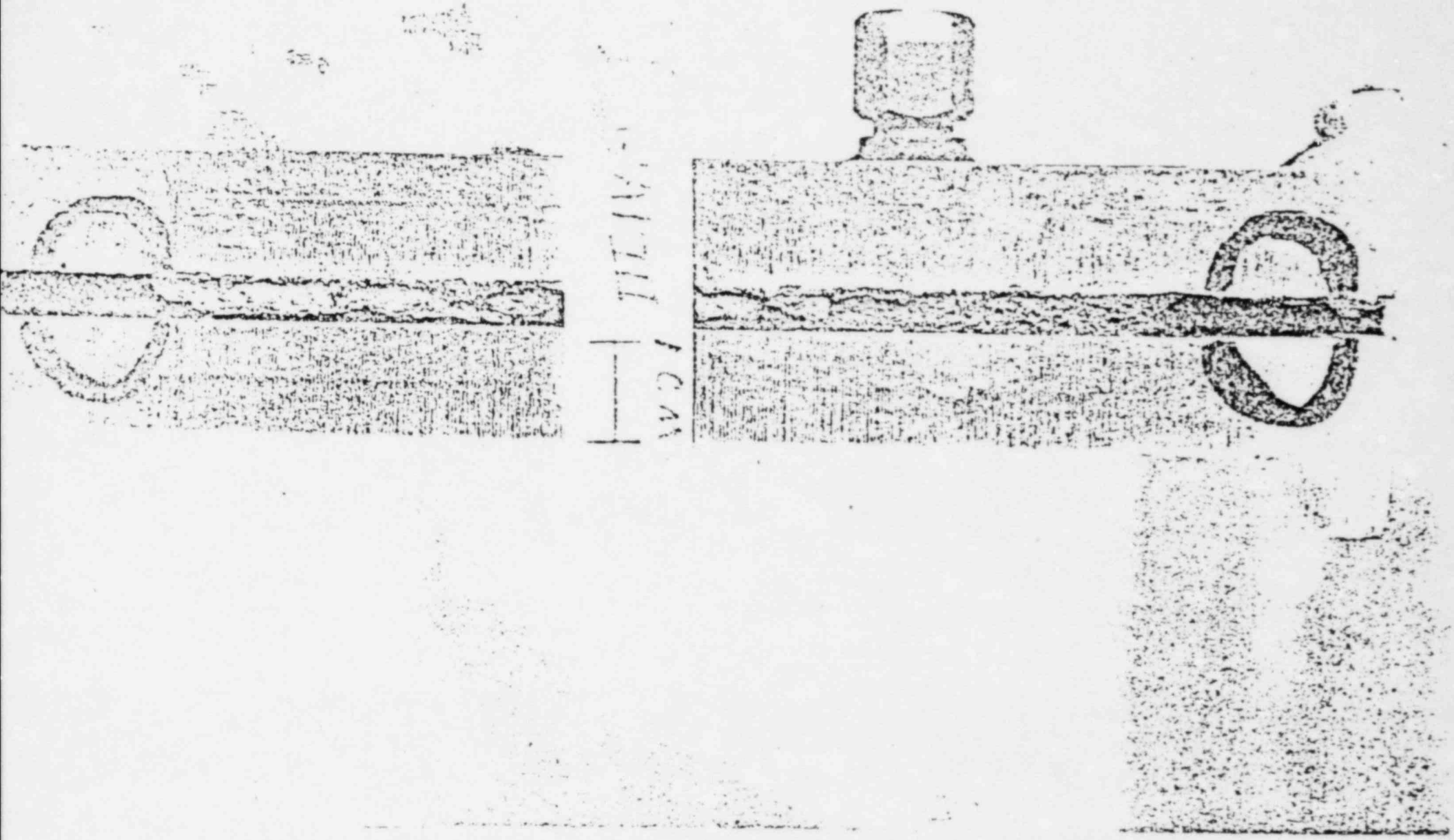

Figure 7. Photograph of Frozen Fuel Debris in GAP-3 Test

B. GAP-4

The GAP-4 test was nominally identical to GAP-3 except that: i) finer uranium powder was selected for a faster burn time, and ii) the settling time was reduced from 3.3 to 0.3 s. Use of the finer mixture resulted in a burntime of 2.86 s compared to 14.3 s for GAP-3. The pressure at the onset of injection was 0.150 MPa (7.0 psig), almost identical to the 0.146 MPa initial injection pressure for GAP-3. In this test, 2.38 kg of molten reaction products entered the gap test section, and the leading edge penetration distance was about twice that for the previous test, 0.35 m. The gammagraph, Fig. 5, shows a significantly different appearance than GAP-3, showing fingers of material which drained down along the walls. Furthermore, the material did not backfill up into the corners, but showed a generally downward and gradually widening flow pattern. The injector was essentially emptied in this test so that all the available fuel was able to enter into the gap. The TC data, Fig. 8, suggests the first hot material penetrated the gap with a velocity of $\sim$ 13.6 m/s.

The test section was cut crosswise at 10.8 and 25.8 cm below the entrance and lengthwise at 1.0 cm off centerline. The cross-section from near the leading edge, Fig. 9, shows that the fuel spans the gap and has macroscopic porosity. It also shows fuel crust layers on the walls. Some localized wall melting was found, particularly near the entrance. Overall, the molybdenum remained uniformly dispersed in the oxide fuel in this test so that this specific objective in rerunning GAP-3 was successfully achieved.

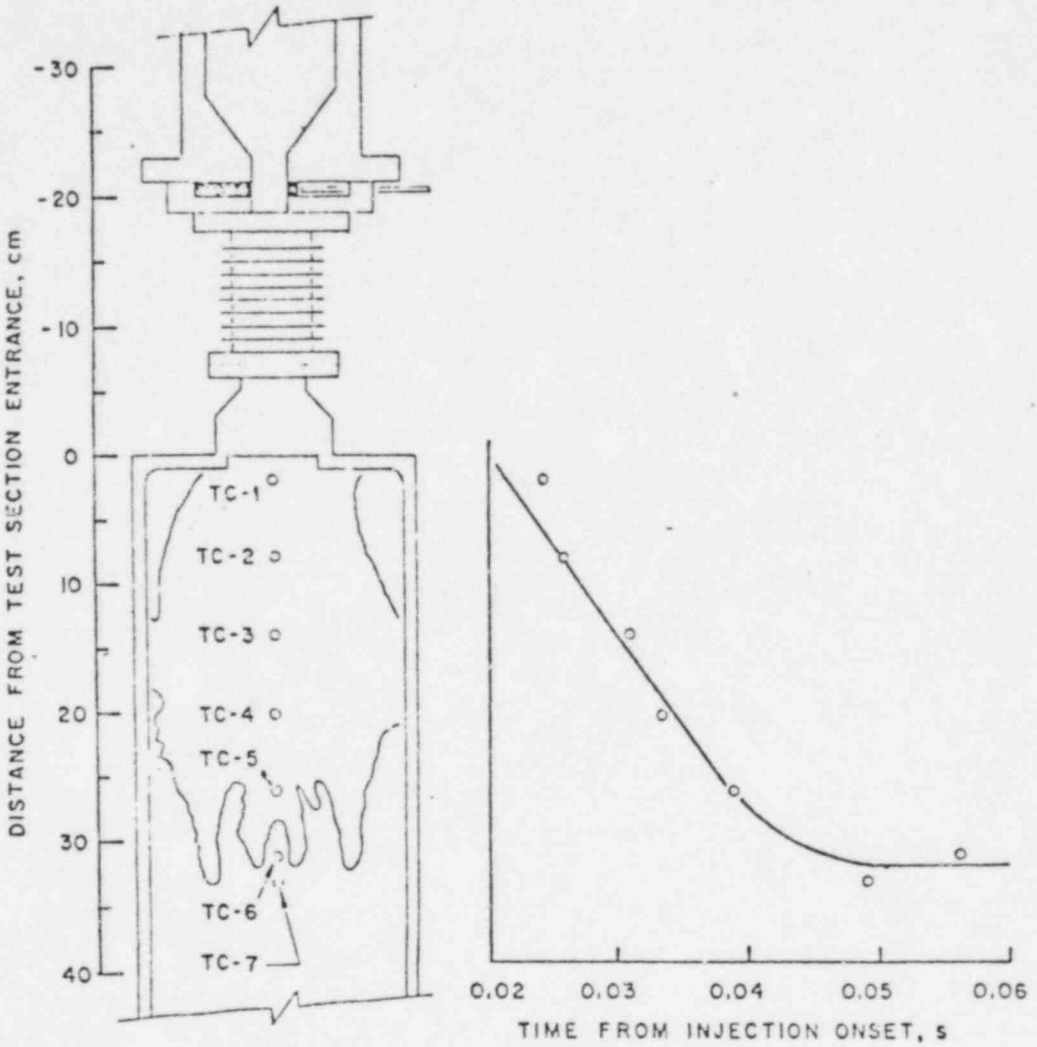

Figure 8. Thermocouple Data from GAP-4 Showing Leading Edge Travel Times

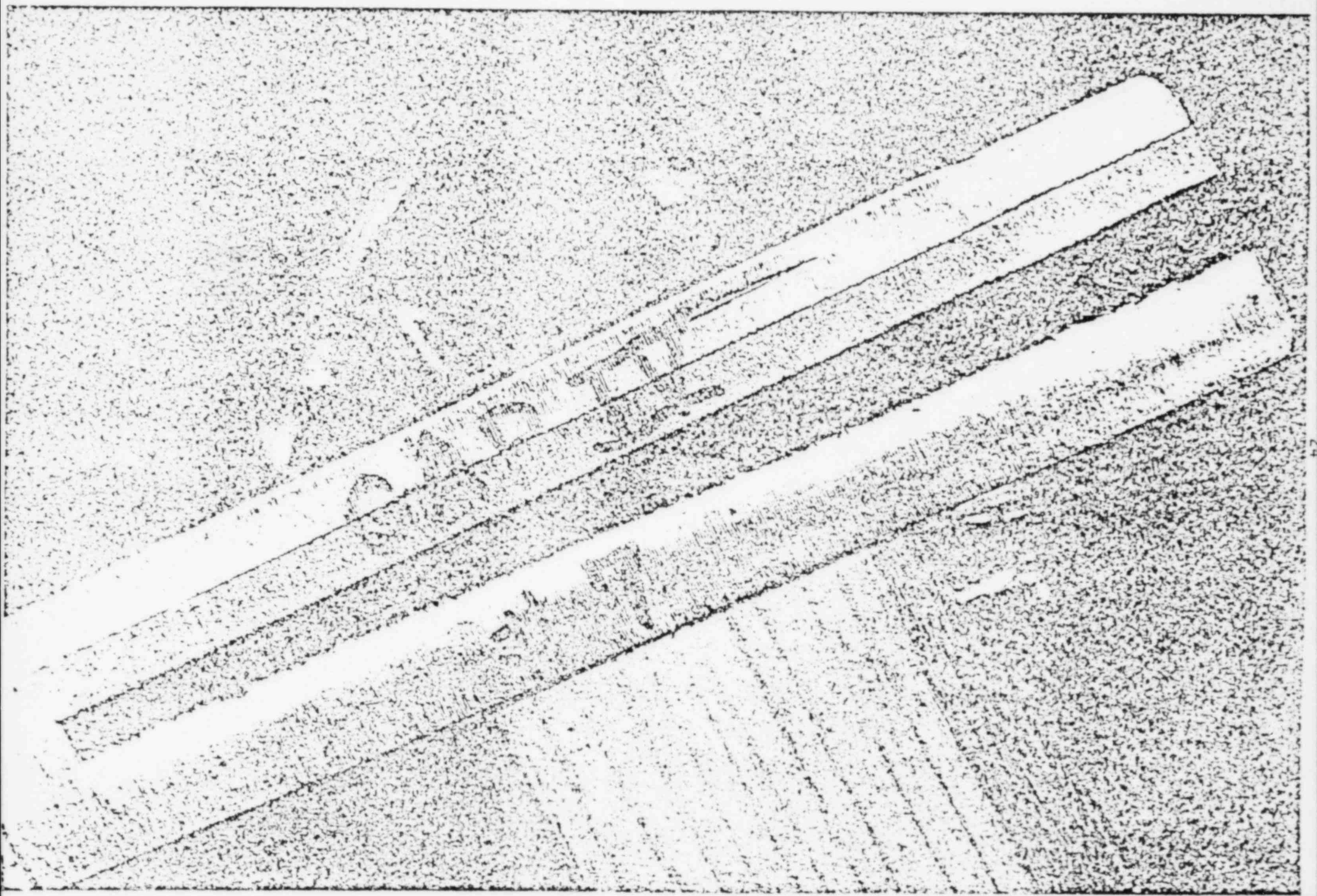

Figure 9. Photograph of Frozen Fuel Debris from Crosscut at x = 0.26 m.

IV. ANALYSIS

Calculations of molten fuel penetration through gap-like flow paths were performed using the computer code EMF-C (Experiment Modeling Freezing Code-Conduction). EMF-C describes the conduction freezing of fuel flowing through a stainless steel circular tube or rectangular channel. For the gap problem, EMF-C models the draining fuel as a one-dimensional, growing length of incompressible liquid flowing through a rectangular channel possessing dimensions which vary in space and time to reflect the growth and remelting of fuel crust. Behind the fuel leading edge, crust formation and conduction heat transfer are modeled normal to the flow assuming a slab geometry which neglects the finite width of the steel channel. For the small gap size under consideration, this is expected to be a good approximation. The one-dimensional calculations of the simultaneous growth of crust and the heating of the surrounding steel combine a continuous tracking of the fluid-crust interface together with a finite difference formulation of conduction heat transfer within the crust and steel. Calculations are continued until either the fuel leading edge reaches the bottom of the channel or the crust grows to completely occlude the flow channel at some location.

Calculations were first performed for the reactor case in which the fuel was considered to be pure UO_2. The calculations assume a rectangular channel possessing a gap size equal to the nominal CRBR inter-subassembly gap (0.43 cm) and a width (6.7 cm) equivalent to the outer periphery of one hexcan flat. The channel has a total length of 146.9 cm equal to the height of the active core (91.44 cm) plus the length of the region between the active core and the shield (55.5 cm). Further penetration through the narrow gaps in the shield and orifice regions is not considered. The steel channel walls are assumed to possess a thickness (0.305 cm) equal to that of driver, control rod, and internal blanket ducts within the heterogeneous core. The channel wall outer surfaces are treated as adiabatic boundaries. Within the active core region, the initial hexcan temperature is taken equal to 1173°K, representative of sodium saturation conditions. Below the core, an initial structure temperature of 660°K is assumed, consistent with the sodium inlet temperature.

The first calculation models the gravity-driven drainage of molten UO_2 initially at its liquidus temperature of 3138°K. The formation of a complete plug is predicted at 2.02 s when the crust growth at the entrance fully occluded the gap. The leading edge penetration distance was 1.23 m. The calculated penetration as a function of time is shown in Fig. 10. The effect of applying a 0.1 MPa (1 atm) pressure drop across the expelled fuel slug is shown in Fig. 11. The fuel leading edge is predicted to transcend the full length of the gap channel in 0.54 s, reaching the shield region with a velocity of 1.51 m/s. At the time of full penetration, the crust at the channel entrance occluded 55% of the gap thickness. Increasing the driving pressure further to 0.5 MPa shortened the full penetration time to 0.22 s, increased the final velocity to 4.23 m/s, and decreased the gap occlusion to 37%.

A calculation was carried out to examine the effects of raising the initial fuel temperature to 3473°K. The result for the gravity drain case is shown in Fig. 12. The fuel is predicted to penetrate the full gap length, reaching the shield block at 1.21 s with a velocity of 1.26 m/s. The maximum gap occlusion for this case was 48%, located near the bottom of the core region.

Additional calculations were performed specifically to support the design of the experiment apparatus. In these cases, the injected thermite material (81% UO_2, 19% Mo at 3473°K) was modeled using thermophysical properties for UO_2 with the exceptions that the thermal conductivity and viscosity were increased to account for the presence of the metallic phase. The calculations assume a rectangular channel possessing a gap size equal to the nominal CRBR intersubassembly gap (0.43 cm) and a width (20.13 cm) equal to the outer periphery of three hexcan flats. The resulting initial flow area and hydraulic diameter are 8.69 cm^2 and 0.85 cm respectively. The channel is assumed to be 1.0 m long and closed at the bottom (downstream) end. A single initial fuel temperature of 3473°K is assumed for the injected fuel at the channel inlet. The initial steel wall temperature was varied between 873°K and 1073°K. To provide adequate long term containment of the fuel enthalpy without melting through the test section, it was necessary

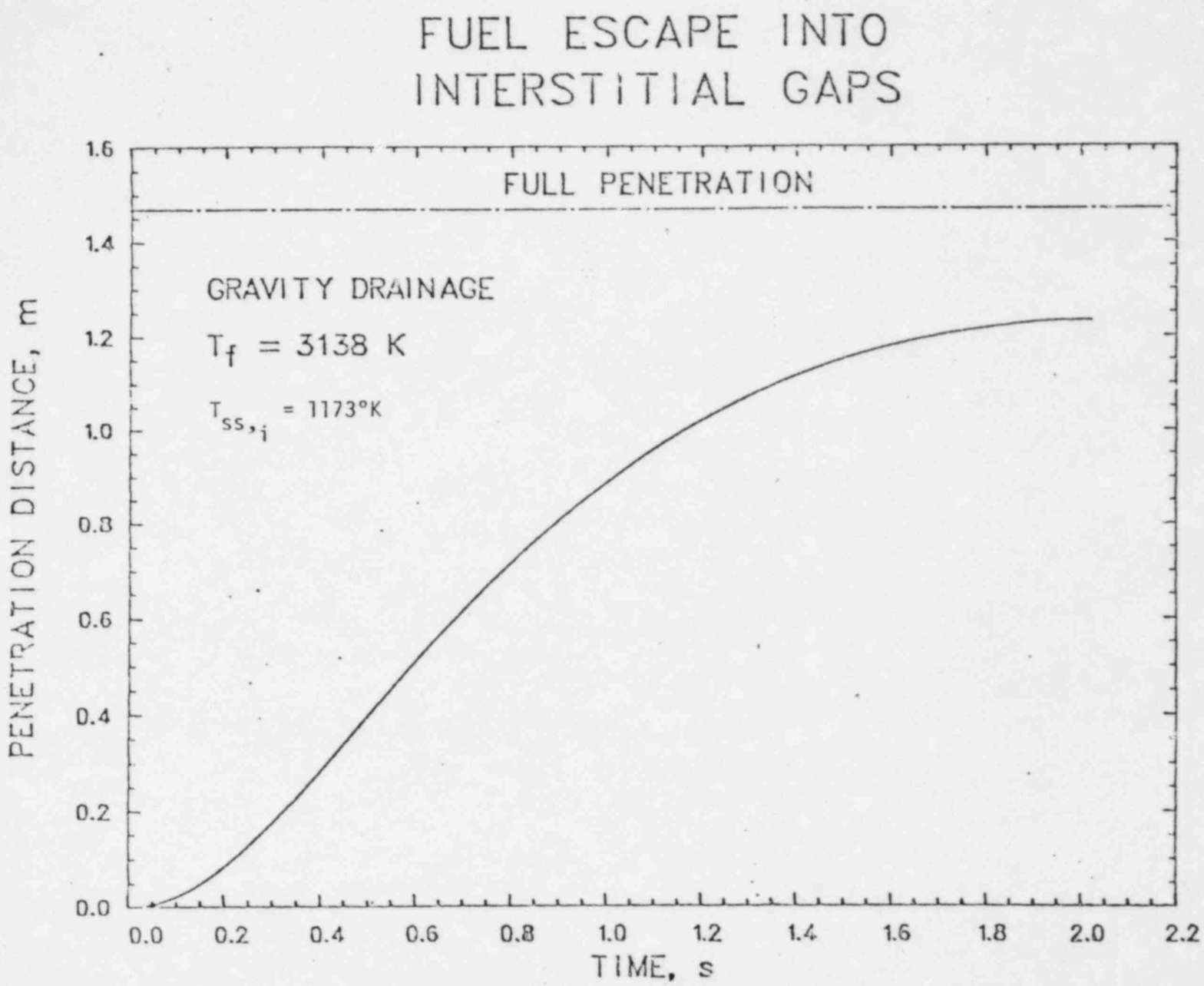

Fig.10. Fuel Leading Edge Penetration Distance Versus Time for Case of Gravity Drainage and Initial Fuel Temperature = 3138 K.

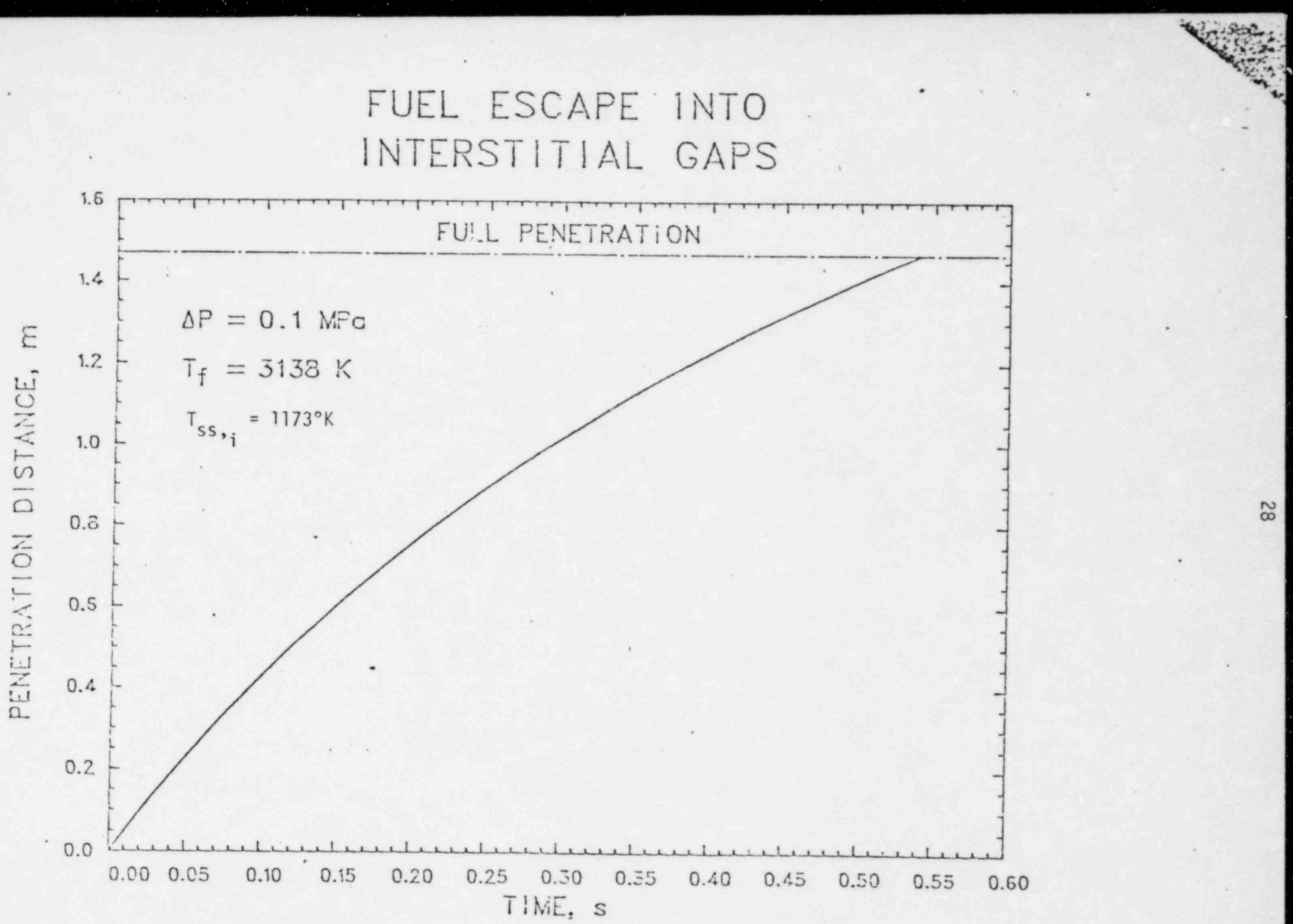

Fig.11. Fuel Leading Edge Penetration Distance Versus Time for Case of Driving Pressure Drop = 0.1 MPa and Initial Fuel Temperature = 3138 K.

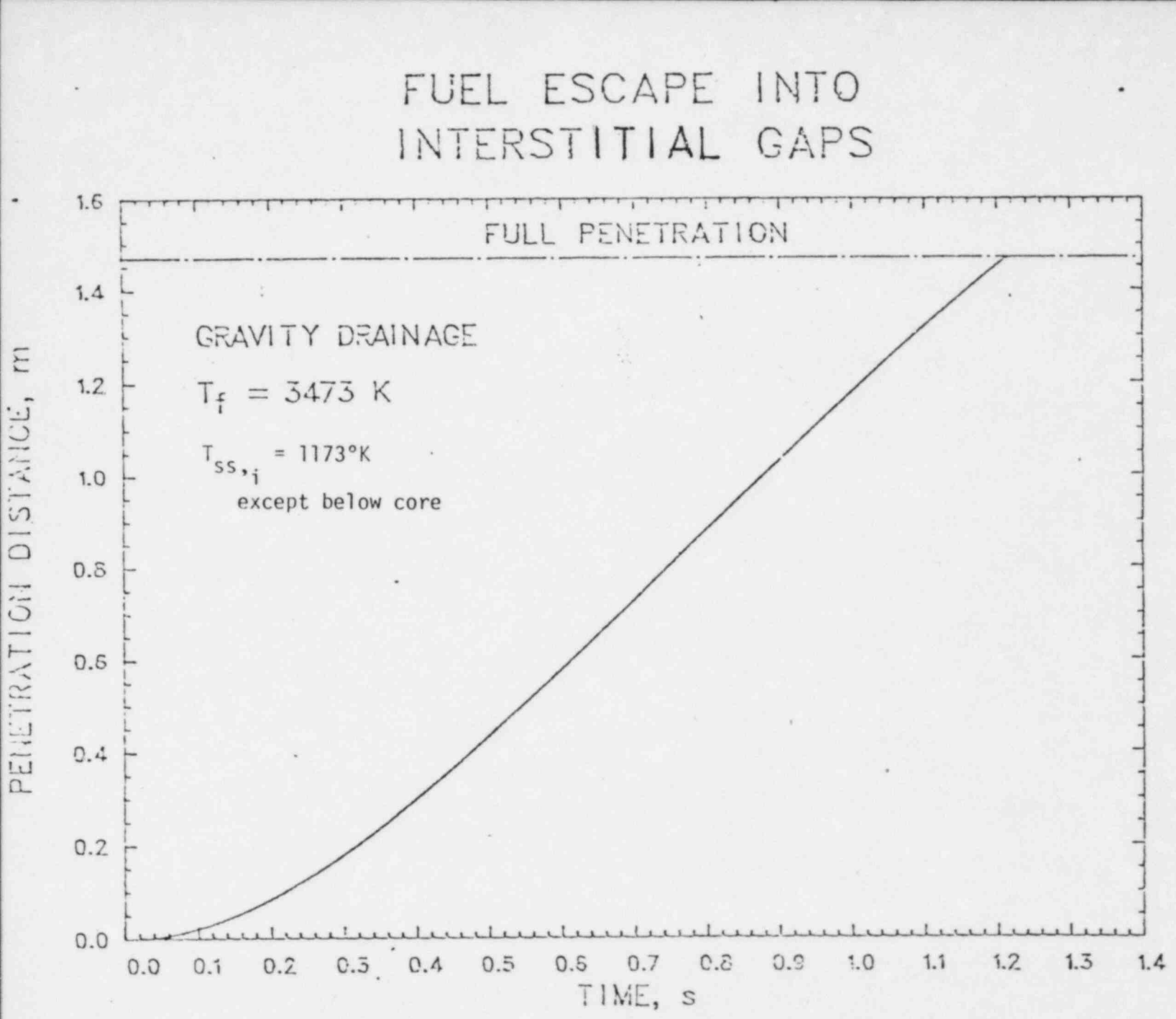

Fig. 12. Fuel Leading Edge Penetration Distance Versus Time for Case of Gravity Drainage and Initial Fuel Temperature = 3473 K.

to employ a steel wall thickness exceeding that of the subassembly hexcan (0.305 cm). A reference value of the test section wall thickness of 0.95 cm (0.375 inch) was used. To assess the effects on fuel penetration of an increased wall thickness for the test section relative to a hexcan in the reactor environment, calculations were carried out for the following three cases:

Case a. The steel wall is assumed to be 0.95 cm thick and the wall outer surface is treated as an adiabatic boundary.

Case b. A steel wall thickness equal to that of the subassembly hex can (0.305 cm) is assumed and the outer surface is treated as an adiabatic boundary.

Case c. The steel wall thickness is equal to that of the hexcan. In addition, it is assumed that a region of stagnant liquid sodium 5.5 cm thick (half of the subassembly inside flat-to-flat distance) surrounds the steel. The objective here is to simulate, in at least a rough manner, the thermal response of sodium postulated to remain within subassemblies below the level of an active core. The calculations assume that the sodium remains stationary and single-phase. Thus, the effects of coolant convection as well as phase change are not modeled.

Figure 13 shows the calculated leading edge penetration distance as a function of time for gravity draining of thermite reactants in the experiment test section (Case a) at an initial steel temperature of 1073°K. The fuel leading edge is predicted to transcent the 1.0 m long flow channel and reach the bottom of the test section at 0.97 s following injection. Sufficient time has not passed for the crust to fully occlude the channel. Figure 14 shows the crust thickness on each wall at the time of complete penetration as a function of the axial distance downward through the test section. The crust is observed to be thickest at a distance of 0.50 m into the test section where 49% of the channel thickness is blocked by the solidified fuel crust. The location of the maximum crust thickness decreases as the initial fuel temperature is lowered and would conincide with the inlet if the fuel were assumed to enter the channel at its liquidus temperature. Despite the assumed

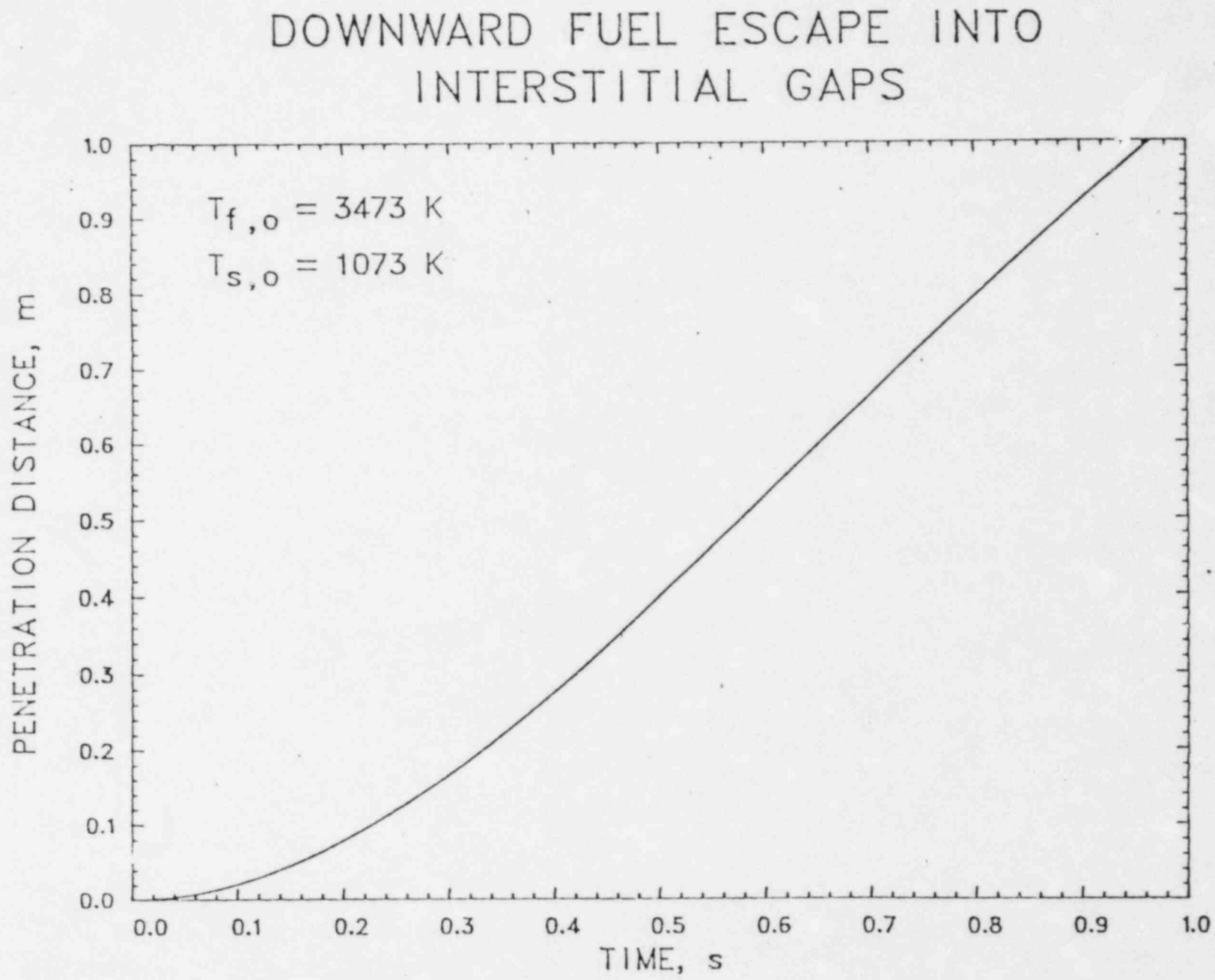

Fig. 13. Leading Edge Penetration Distance Versus Time for an Initial Steel Temperature of 1073 K.

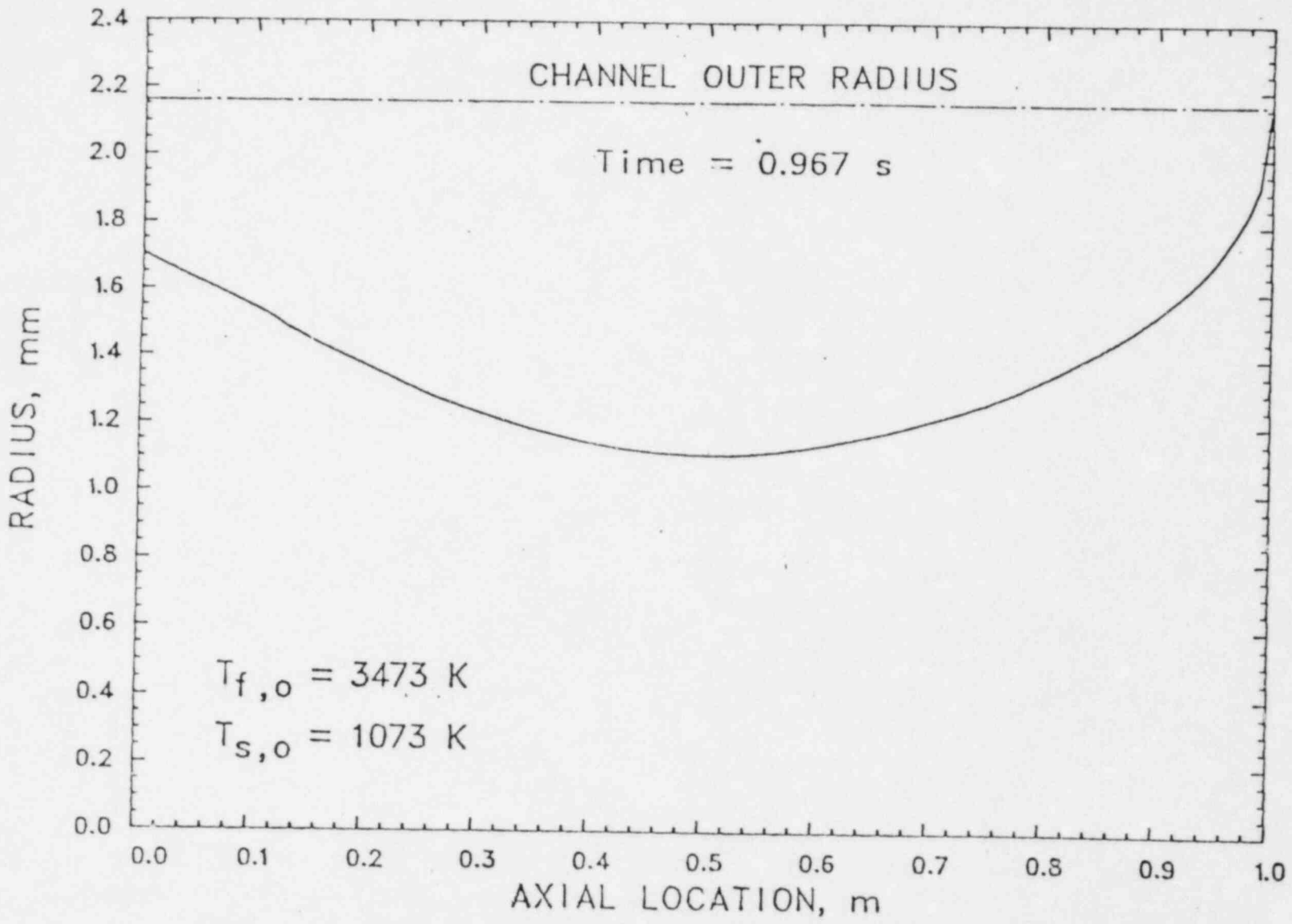

Fig. 14. Crust Profile at the Time of Full Penetration for an Initial Steel Temperature of 1073 K.

presence of a stable fuel crust as well as a thick steel wall, melting of steel is calculated to occur prior to full penetration. Steel melting is first calculated at the inlet shortly before 0.7 s when the leading edge penetration distance is 0.65 m and the corresponding injected mass over one subassembly flat width is 1.63 kg. At the time of complete penetration, steel melting has commenced over the first 11 cm beyond the channel inlet. The melting attack is most severe at the inlet where 7% of the wall thickness is molten or in the process of melting. The calculation assumes that molten steel remains stationary between the crust and remaining unmelted steel. Major uncertainties here include the continued stability of fuel crust when the steel substrate undergoes melting as well as the mechanical deformation and failure of the surrounding steel under the calculated thermal loading.

The time dependent fuel penetration, crust growth and the thermodynamic state of the flowing molten fuel were found to be insensitive to the steel wall thickness and the wall outer boundary condition as scoped by Cases a-c. Indeed, the penetration times for a 1 m distance predicted for Cases b and c are exactly equal to that obtained for Case a. For all three cases, virtually identical crust profiles are calculated. In contrast to the calculated fuel behavior, differences in the thermal response of the steel structure were observed between Case b (hexcan wall thickness, adiabatic outer surface) and Cases a and c. This is illustrated by Fig. 15 which shows the temperatures within the steel at the channel inlet at the time of complete penetration for the three cases. It is observed that the thick steel wall of the test section provides a very good simulation of a hexcan surrounded by stationary liquid sodium, especially as the fuel-steel interface is approached. This is an important result, since sodium would be expected to remain in subassemblies below the core in the loss-of-flow scenario. For Cases a and c, similar steel melting behavior is obtained. However, for Case b, higher steel wall temperatures and a greater degree of steel melting are calculated. At the time of full penetration, melting has commenced over the first 14 cm beyond the channel inlet. It is observed from Fig. 15 that at the time of full penetration, the thermal boundary layer has just penetrated

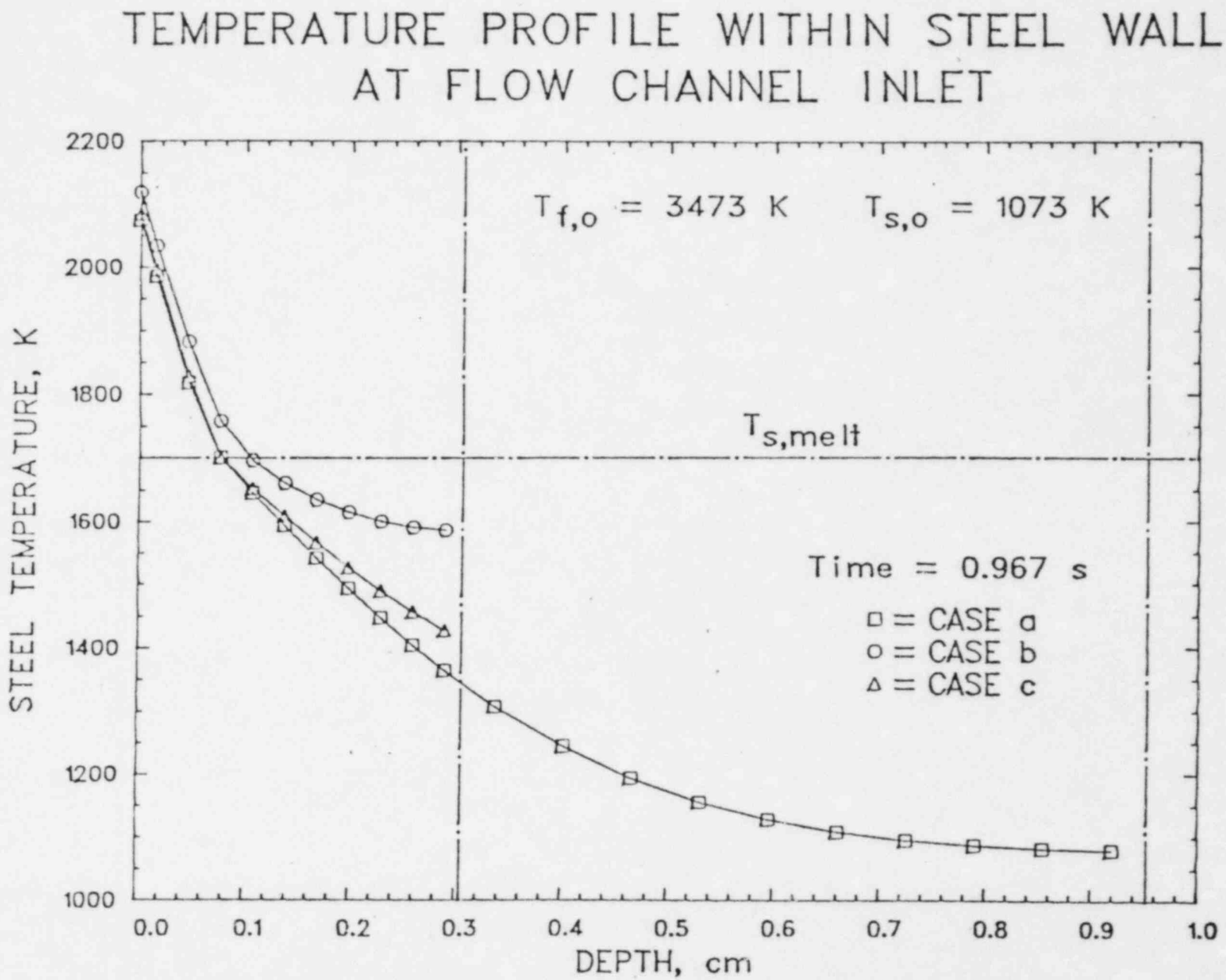

Fig. 15. Temperatures Within Steel Wall at the Flow Channel Inlet at the Time of Full Penetration for an Initial Steel Temperature of 1073 K.

the full steel wall thickness in the experiment test section cases. Thus, the assumed wall thickness (0.95 cm) constitutes an essentially infinite wall from a thermal standpoint over the time scale of fuel drainage.

The following were concluded from the pretest analytical study:

i) The molten thermite material would be expected to drain the full 1 m length of the test section.

ii) The thermite penetration through the gap geometry is insensitive to the presence of additional heat capacity beyond the hexcan thickness; hence the nominal 1 cm thickness needed for structural rigidity and long-term containment would not introduce anomolous boundary effects.

iii) The wall melting would be somewhat less for the test section wall thickness than for the case of the voided hexcan; however, the wall melting behavior would be nearly identical to that for a nonvoided hexcan.

REFERENCES

1. B.W. Spencer, et al., "Reactor-material Fuel-freezing Experiments Using Small-bundle, CRBR-type Pins, ANL-80-22 (1980).

2. B.W. Spencer, et al., "Summary and Evaluation of Reactor-material Fuel Freezing Tests, " Proc. Intl. Mtg. Fast Reactor Safety Technology, Seattle, WA, Aug. 19-23, 1979.

3. B.W. Spencer and D.H. Cho, "Phenomenological Studies of HCDA Issues," Proc. Intl. Topical Mtg. on LMFBR Safety, Lyon, France, July 19-23, 1982.

4. S.K. Rhow, et al., "An Assessment of HCDA Energetics in the CRBR Heterogeneous Reactor Core, " CRBRP-GEFR-00523 (1981).

5. D.M. Switick, General Electric Co., private communication.

6. ANL/RAS Report re: Hexduct Rupture Tests, in preparation.